Environment International 217 (2026) 110586



Contents lists available at ScienceDirect

Environment International

journal homepage: www.elsevier.com/locate/envint



Full length article

Assessing the health and economic burden of sick leave associated with long-term fine particulate matter exposure: a 13-year analysis using German health claims data

Benjamin Aretz [a,b,*], Jonas Böcker [a], Michael Arz [a], Lorenza Gilardi [c], Matthias Schmid [b], Michael Bittner [c], Jörn Rittweger [a,d,1]

[a] Institute of Aerospace Medicine, German Aerospace Center (DLR), Cologne, Germany
[b] University of Bonn, University Hospital Bonn, Institute for Medical Biometry, Informatics and Epidemiology (IMBIE), Bonn, Germany
[c] German Remote Sensing Data Center, German Aerospace Center (DLR), Oberpfaffenhofen, Germany
[d] Department of Pediatrics and Adolescent Medicine, University Hospital Cologne, Cologne, Germany

ARTICLE INFO

Keywords:
Ambient $PM_{2.5}$exposure
Sick-leave burden
Productivity losses
Exposure-response curve
Generalized additive models
Environmental epidemiology

ABSTRACT

Background: Ambient fine particulate matter ($PM_{2.5}$) is a major environmental health risk, yet its contribution to sick leave and related productivity losses remains insufficiently quantified. We therefore examined the association between $PM_{2.5}$ exposure and all-cause sick leave days and estimated the corresponding model-based burden and productivity losses.

Methods: Using routine health insurance data from AOK Baden-Württemberg for 2010–2022, we fitted generalized additive models with penalised splines to estimate the exposure–response curve between monthly $PM_{2.5}$ exposure and all-cause sick leave days. Models were adjusted for long-term trends, seasonality, temperature, sex, the COVID-19 period, NO_2, vacation days, and lockdown days, and accounted for spatial heterogeneity using a postal-code-based Markov random field. Model-based exposure contrasts were derived from predicted sick leave days at selected $PM_{2.5}$ concentrations. Productivity losses were estimated using the human capital approach.

Results: $PM_{2.5}$ showed a positive non-linear association with sick-leave days ($p < 0.001$). Compared with 5 μg/m^3, adjusted predicted sick-leave days were 9.56% higher at 10 μg/m^3 (95% CI 9.09–10.00) and 15.00% higher at 20 μg/m^3 (95% CI 14.20–15.80), while little change was observed between 10 and 15 μg/m^3 (+0.04%, 95% CI − 0.30 to 0.38). The overall non-linear association was supported across additional analyses, although its magnitude and precise shape varied with temporal coverage and covariate adjustment. $PM_{2.5}$ concentrations above the WHO guideline of 5 μg/m^3 corresponded to 105 model-attributable excess sick-leave days per 1,000 working-age inhabitants per year, equivalent to approximately 5.31 million excess sick-leave days and €1.56 billion in annual productivity losses in Germany.

Conclusion: Higher $PM_{2.5}$ exposure was associated with a relevant model-attributable burden of sickness absence and productivity losses. These findings suggest that ambient $PM_{2.5}$ may be an important population-level correlate of work absence, although causal interpretation is limited by the ecological study design and residual confounding.

1. Background

Sick leave is a major public health and economic concern, as it reflects both the population's underlying health status and the economic burden of productivity loss due to illness (Gabbay et al., 2011; The Lancet Public Health, 2018). In Germany, the average number of sick-leave days per employee nearly doubled from 8.1 days in 2007 to 15.1 days in 2023 (Destatis, 2025c).

Despite the societal relevance of sickness absence, its environmental determinants remain insufficiently understood. Workplace-related factors explain only part of the burden, with physical work environment exposures accounting for approximately 10–30% of sickness absence

* Corresponding author at: Institute of Aerospace Medicine, German Aerospace Center (DLR), 51147 Cologne, Germany.
E-mail address: benjamin.aretz@dlr.de (B. Aretz).
[1] Deceased prior to publication.

https://doi.org/10.1016/j.envint.2026.110586
Received 21 July 2026; Received in revised form 12 October 2026; Accepted 28 October 2026
Available online 1 November 2026
0160-4120/© 2026 The Authors. Published by Elsevier Ltd. This is an open access article under the CC BY license (http://creativecommons.org/licenses/by/4.0/).
Open access funding enabled and organized by Projekt DEAL.

(Bang Christensen et al., 2007). Meanwhile, growing evidence suggests that regional and environmental characteristics also contribute to sickness absence (Blomgren, 2015; Kriit et al., 2024; Reuter et al., 2020).

Among these environmental determinants, fine particulate matter with an aerodynamic diameter of ≤2.5 μm ($PM_{2.5}$) is one of the leading environmental health hazards worldwide. Short-term $PM_{2.5}$ exposure has been estimated to contribute to approximately 1 million premature deaths annually worldwide, while in Germany long-term exposure was associated with about 27,000 deaths and 569,000 disability-adjusted life years in 2019, underscoring its substantial population-level health burden (Yu et al., 2024a; Hahad et al., 2025).

Beyond mortality and disability-adjusted life years, $PM_{2.5}$ has been linked to a range of health outcomes that may plausibly translate into sickness absence, including respiratory viral infections, acute cardiovascular events, and exacerbations of chronic respiratory conditions such as asthma and chronic obstructive pulmonary disease (Li et al., 2022; Sangkham et al., 2024; Tahara et al., 2021). Mechanistic evidence suggests that both short- and long-term $PM_{2.5}$ exposure can impair respiratory and systemic health through altered epithelial barrier function, immune dysregulation, airway and systemic inflammation, oxidative stress, and cardiovascular stress (Aretz et al., 2021; Aretz et al., 2024; Krittanawong et al., 2023; Ma et al., 2024; Zhai et al., 2022). These mechanisms may increase susceptibility to infection and exacerbate pre-existing disease, thereby reducing functional capacity and increasing the likelihood of sickness absence. Consistent with this, higher ambient $PM_{2.5}$ exposure has been associated with increased incidence and severity of viral respiratory illnesses such as influenza across both rural and urban settings (Brocke et al., 2025; Hsiao et al., 2022; Orr et al., 2025; Rittweger et al., 2022), and recent evidence also suggests associations with SARS-CoV-2 infection and related outcomes (Hoffmann et al., 2025; Lin et al., 2025; Yu et al., 2024b).

However, evidence linking ambient $PM_{2.5}$ exposure to sickness absence remains scarce and has so far focused predominantly on short-term exposure. In Stockholm, Kriit et al. (2024) reported an 8.5% increase in the odds of initiating a sick-leave episode per 10 $\mu g/m^3$ increase in $PM_{2.5}$ exposure 2–4 days earlier. More recently, Mahakalkar et al. (2026) examined short-term air-pollution exposure and acute health outcomes in Baden-Württemberg using AOK health-insurance data and a case-crossover design. These studies address whether transient increases in air pollution act as acute triggers of sickness absence or related health events.

A complementary question is whether longer-term regional $PM_{2.5}$ exposure, represented by monthly mean concentrations over an extended observation period, is associated with the overall burden of sickness absence. Such an approach captures a different dimension of exposure than short-term analyses, reflecting persistent regional exposure patterns rather than day-to-day pollution peaks, and is particularly relevant for estimating population-level burden and associated productivity losses. To our knowledge, this longer-term association between $PM_{2.5}$ exposure and sickness absence has not been quantified using large-scale routine health-insurance data over an extended observation period.

We therefore examined the association between monthly $PM_{2.5}$ exposure and all-cause sick-leave days across Baden-Württemberg during a 13-year observation period and quantified the associated sick-leave burden and productivity losses. Specifically, we aimed to characterise the potentially non-linear exposure–response relationship and to estimate the corresponding model-based population-level burden of sickness absence. Baden-Württemberg provides a suitable setting because comprehensive AOK health-insurance data are available across both urban and rural regions, allowing spatially resolved linkage with environmental exposure estimates.

2. Methods

2.1. Study population and setting

The study was conducted in Baden-Württemberg, Germany, using routine health insurance data from AOK Baden-Württemberg, one of the regional statutory health insurance funds within the German healthcare system. Baden-Württemberg has approximately 11 million inhabitants, of whom around 4.5 million are insured with AOK Baden-Württemberg. The state includes highly urbanised and industrialised areas as well as rural regions, providing substantial spatial heterogeneity in population structure and environmental exposures.

The analytical population comprised all AOK-insured individuals of working age (18–64 years) residing in Baden-Württemberg between January 2010 and December 2022. In Germany, statutory health insurers routinely receive information on certified sickness absence because physicians issue certificates of incapacity for work that are transmitted for administrative and reimbursement purposes. Accordingly, AOK routine data include records of certified sick-leave episodes and their duration in addition to healthcare utilisation and diagnostic information. For the present study, data were provided exclusively in aggregated form to comply with applicable data-protection requirements.

The study was conducted in accordance with the Declaration of Helsinki and approved by the Ethics Committee of the Medical Council (Landesärztekammer Nordrhein) within the VARIAQ study (reference number 2020092). Data management procedures were reviewed and approved by the data protection officers of both the German Aerospace Center (DLR) and AOK before data exchange.

2.2. Sick leave data

We used administrative data from the AOK sick-leave database, which captures certified sick-leave episodes and their duration across space and time. The sick–leave data were provided by AOK in aggregated form. The aggregation was performed at the level of five-digit postal code (PLZ) and date. This corresponds to the spatial and temporal resolution of the environmental exposure data. The dataset includes, for each aggregation group, the count of new sick–leave cases and the mean duration of those cases (individual case durations Winsor–capped at 60 days).

2.3. Air pollution and temperature data

Ambient $PM_{2.5}$ and NO_2 (nitrogene dioxide) concentrations were obtained from the Copernicus Atmosphere Monitoring Service (CAMS) European air quality reanalysis for 2010–2022 (Marécal et al., 2015; Copernicus Atmosphere Monitoring Service, 2021). The CAMS reanalysis combines chemical transport modelling with ground-based observations through data assimilation and provides hourly surface-level pollutant concentrations at a horizontal resolution of $0.1^\circ \times 0.1^\circ$ (approximately 10 km). $PM_{2.5}$ was the primary exposure of interest, while NO_2 was included as a potential confounder. Air temperature was obtained from the ERA5-Land reanalysis dataset (Copernicus Climate Change Service, 2019), which has the same nominal spatial resolution.

$PM_{2.5}$ and NO_2 concentrations were spatially aggregated to five-digit postal code areas. To reduce sensitivity to arbitrary raster-cell assignment along irregular postal-code boundaries, the native CAMS fields were bilinearly resampled to a finer computational grid before calculating area-weighted postal-code means. This procedure improves spatial allocation at polygon boundaries but does not increase the underlying spatial information of the original CAMS data. Postal-code-level hourly concentrations were subsequently aggregated to daily and then monthly, quarterly, and yearly means to match the temporal structure of the health data.

2.4. Statistical analysis

Sick-leave burden was described using the number of sick-leave episodes and the total number of sick-leave days in relation to the number of AOK-insured individuals within each postal-code area and time unit.

For descriptive spatial analyses, annual sick-leave episodes and sick-leave days were calculated per AOK-insured individual for each five-digit postal code area. Spatial patterns were described for four selected years representing distinct phases of the study period: 2010, the first year of observation; 2019, the last pre-pandemic year; 2021, a year still characterised by substantial COVID-19-related restrictions; and 2022, the final study year, when most pandemic-related restrictions had been lifted and electronic sick-leave reporting had become more widely implemented. This selection was intended to illustrate spatial patterns across major temporal transitions rather than to provide an exhaustive year-by-year comparison. Temporal patterns were examined at yearly, monthly, daily, and weekday resolutions. For short-term temporal analyses, 30-day sick-leave incidence rates were calculated as the number of sick-leave episodes within a 30-day period divided by the corresponding population at risk and multiplied by 1,000.

The association between $PM_{2.5}$ exposure and sick-leave days was analysed using generalized additive models. Models were fitted using a negative binomial distribution with a log link and included the logarithm of the number of insured individuals as an offset. The primary analysis was conducted at the monthly postal-code level. This temporal resolution was chosen to capture longer-term regional exposure patterns rather than short-term day-to-day pollution fluctuations, which have been examined separately in previous case-crossover work in the same region. Penalised splines were used for $PM_{2.5}$ and temperature to allow flexible non-linear relationships without imposing a predefined functional form. Spatial heterogeneity was accounted for using a Markov random field defined by the neighbourhood structure of five-digit postal-code areas (Wood, 2017). The complete model specification is given below:

$$g(E[Y_{zt}]) = \beta_0 + f_{PM(PM_{2.5,zt})} + \beta_1 year_t + \beta_2 sex_z + \beta_3 PandemicPeriod_t + \beta_4 NO_{2,zt} + f_{T(temperature_{zt})} + \beta_5 VacationDays_{zt} + \beta_6 LockdownDays_{zt} + \gamma_{time(t)} + s_{MRF(z)} + (\log(N_{zt}))$$

where $g(\cdot)$ denotes the log link function, Y_{zt} the number of sick-leave days in postal-code area (z) and time unit (t), and N_{zt} denotes the number of AOK-insured individuals in the respective postal-code area and time unit. The term $\log(N_{zt})$ was included as an offset. f_{PM} denotes the penalised exposure–response function for $PM_{2.5}$ concentration (μg/m^3), f_T the penalised smooth function for temperature (°C), and $s_{MRF(z)}$ the Markov random field term capturing spatial dependence between neighbouring postal-code areas. $NO_{2,zt}$ denotes ambient NO_2 concentration (μg/m^3).

$VacationDays_{zt}$ and $LockdownDays_{zt}$ denote the number of vacation and lockdown days within the respective time unit. Vacation days were derived from the official school-holiday calendars for Baden-Württemberg published by the Standing Conference of the Ministers of Education and Cultural Affairs of the Länder in the Federal Republic of Germany (KMK, 2026). Lockdown days were derived from the IAB Data Base on Coronavirus Containment Measures (IAB, 2023; Bauer and Weber, 2021), which provides daily information on COVID-19 containment measures by German federal state and, where applicable, district. For each time unit, the respective number of vacation and lockdown days was calculated and included as a time-varying covariate.

Finally, $\gamma_{time(t)}$ denotes the seasonal effect, modelled using orthogonal polynomial contrasts, e.g., contrasts of quarters in the quarterly models or calendar month in the monthly models (Chambers 1997).

Because $PM_{2.5}$ was modelled using a penalised smooth term, no single global coefficient for the $PM_{2.5}$ effect can be directly interpreted. We therefore derived model-based exposure contrasts from average adjusted predictions of the fitted GAM. Specifically, $PM_{2.5}$ was set to 5, 10, 15, and 20 μg/m^3, while all other covariates were kept at their observed values. These concentrations were selected a priori to provide interpretable contrasts across the central exposure range observed in the study population, with 5 μg/m^3 corresponding to the WHO annual air quality guideline and the remaining values representing equally spaced 5-μg/m^3 increments up to 20 μg/m^3. Predicted sick-leave rates were obtained on the response scale by back-transforming the linear predictor, $\exp(X\beta)$, and then averaged across the study population. Relative changes were expressed as percentage differences between these average predicted rates. 95% confidence intervals were derived from 10,000 simulations of the coefficients based on the estimated covariance matrix of the fitted GAM.

To estimate model-attributable sick-leave days associated with $PM_{2.5}$ exposure, observed $PM_{2.5}$ concentrations were compared with a counterfactual scenario in which $PM_{2.5}$ was set to 5 μg/m^3, corresponding to the WHO air quality guideline value for the annual mean $PM_{2.5}$ concentration (World Health Organization, 2021). Predictions were obtained on the response scale, and model-attributable sick-leave days were defined as the excess number of predicted sick-leave days under observed $PM_{2.5}$ concentrations compared with the counterfactual scenario in which $PM_{2.5}$ was set to 5 μg/m^3. Productivity losses were estimated using the human capital approach (Zhang et al. 2011), which values lost work time by assigning a monetary value to each excess sick-leave day. First, the estimated number of excess sick-leave days per 1,000 working-age inhabitants per year was applied to the working-age population of Baden-Württemberg to quantify the burden within the study region. The total annual number of model-attributable excess sick-leave days in Baden-Württemberg was calculated as

$$D_{PM_{2.5}BW} = D_{1,000} \times \frac{N_{BW}}{1,000}$$

where $D_{PM_{2.5}BW}$ denotes the total annual number of model-attributable excess sick-leave days associated with $PM_{2.5}$ exposure in Baden-Württemberg, $D_{1,000}$ the estimated number of excess sick-leave days per 1,000 working-age inhabitants per year, and N_{BW} the number of working-age inhabitants in Baden-Württemberg in 2024 (Statistisches Landesamt Baden Württemberg 2025).

For comparison, we additionally performed a scenario-based extrapolation to the German working-age population. This extrapolation assumes that the estimated burden rate observed in Baden-Württemberg is applicable to the German working-age population as a whole. The corresponding number of model-attributable excess sick-leave days in Germany was calculated as

$$D_{PM_{2.5}GER} = D_{1,000} \times \frac{N_{GER}}{1,000}$$

where $D_{PM_{2.5}GER}$ denotes the scenario-based estimate of the total annual number of model-attributable excess sick-leave days associated with $PM_{2.5}$ exposure in Germany and N_{GER} the number of working-age inhabitants in Germany as of 31 December 2024 (N_{GER} = 50,597,024) (Destatis, 2026).

Second, average daily labour costs were calculated from official statistics of the Federal Statistical Office (Destatis). Annual productivity losses were estimated by multiplying the corresponding number of model-attributable excess sick-leave days by the average daily labour cost:

$$L = D_{PM_{2.5}} \times C_{day}$$

where L denotes annual productivity losses, $D_{PM_{2.5}}$ the number of model-attributable excess sick-leave days, and C_{day} the average daily labour cost. Average daily labour costs were calculated as

$$C_{day} = \frac{W_{month} \times f_{ssc}}{d_{work}}$$

where W_{month} denotes the average gross monthly earnings of full-time employees in Germany in 2024 (W_{month} = €4,701) (Destatis, 2025c), f_{ssc} the factor accounting for employer social security contributions (f_{ssc} = 1.29), and d_{work} the assumed number of working days per month (d_{work} = 20.7) (Destatis, 2024). The same labour-cost estimate was applied to the Baden-Württemberg and Germany calculations to ensure comparability of the regional and national burden estimates.

Sensitivity analyses were conducted using alternative temporal aggregations, including weekly and quarterly models, to assess the robustness of the estimated $PM_{2.5}$ exposure–response function. In addition, we refitted the monthly model using alternative specifications of the temporal component, including modelling calendar year as a spline, adding time since pandemic start, and including a year × COVID interaction (**Supplementary Table e4**). Additional sensitivity analyses were performed to assess whether the estimated non-linear $PM_{2.5}$ association was sensitive to the COVID-19 period or adjustment for NO_2. First, the primary monthly model was refitted after excluding all observations from 2020 to 2022; because the COVID-period indicator and lockdown days showed no variation in the resulting 2010–2019 dataset, these terms were omitted from this model. Second, the primary model was refitted without NO_2 to assess the influence of adjustment for the moderately correlated co-pollutant. Finally, exploratory sex-specific analyses were conducted by fitting separate penalised $PM_{2.5}$ smooths for women and men within a common model using a shared smoothing parameter. Sex-specific model-based exposure contrasts were derived using the same population-standardisation approach as in the primary analysis (**Supplementary Table e5**).

All analyses were performed in R 4.4.2. Generalized additive models fitted with the bam function from the R package *mgcv* to accommodate the large aggregated dataset. Maps and figures were produced using *ggplot2*.

3. Results

3.1. Descriptive characteristics of the study population and exposures

Table 1 summarises the main characteristics of the monthly analytic dataset for the overall study period and selected years, while complete year-specific descriptive statistics are provided in **Supplementary Table e1**. Overall, the study comprised 371,904 aggregated observation units from 1,192 five-digit postal-code areas between 2010 and 2022. The average monthly number of AOK-insured working-age individuals was 2,279,780 and increased from 1,839,258 in 2010 to approximately 2.49 million in 2021 and 2022.

Across all monthly postal-code observations during the study period, the weighted mean $PM_{2.5}$ concentration was 10.42 μg/m^3 (SD 3.53), with a median of 9.64 μg/m^3 (IQR 7.91–12.21). Corresponding values for NO_2 were 12.59 μg/m^3 (SD 5.86) and 11.79 μg/m^3 (IQR 7.93–16.37), respectively. $PM_{2.5}$ and NO_2 were moderately correlated (weighted r = 0.587). Mean temperature was 10.05 °C (SD 6.88), with a median of 9.74 °C (IQR 4.13–16.23). Vacation days averaged 7.46 days per month (SD 8.22; median 6.00, IQR 1.00–10.00), while lockdown days averaged 1.55 days per month across the full study period and 8.62 and 9.85 days per month in 2020 and 2021, respectively. $PM_{2.5}$ concentrations were generally lower in later years than at the beginning of the study period.

3.2. Descriptive patterns of sick leave

Across the full study period, the average monthly burden of all-cause sickness absence was 1,243.89 sick-leave days per 1,000 insured persons. The corresponding average monthly rates were 993.08 in 2010, 1,327.01 in 2019, and 1,784.95 in 2022.

The 30-day incidence of sick-leave episodes per 1,000 inhabitants also increased between 2010 and 2022, with the largest increase occurring between 2021 and 2022 (Fig. 2A). Clear temporal variation was observed: incidence was highest in February and lowest in August and was generally higher between October and March (Fig. 2B). Within months, incidence was lower at the beginning and end of the month (Fig. 2C), while sick-leave episodes were most frequent on Mondays and least frequent on Saturdays and Sundays (Fig. 2D).

3.3. Spatial patterns of $PM_{2.5}$ exposure and sick leave

$PM_{2.5}$ concentrations showed spatial variation across Baden-Württemberg and were generally higher in 2010 than in the subsequently selected years (Fig. 1A–D). Elevated concentrations were mainly observed in northern Baden-Württemberg in 2010, 2019, and 2021, whereas in 2022 higher concentrations were confined to fewer localised

Table 1
Descriptive characteristics of the monthly analytic dataset (overall and selected years).

Characteristic	Overall	2010	2019	2021	2022
Average monthly AOK-insured population	2,279,780	1,839,258	2,481,238	2,489,873	2,489,526
Observation units, n	371,904	28,608	28,608	28,608	28,608
Postal-code areas, n	1,192	1,192	1,192	1,192	1,192
All-cause sick-leave days per 1,000 insured/ month	1243.89	993.08	1327.01	1197.77	1784.95
$PM_{2.5}$, mean (SD), μg/m^3	10.42	12.17	9.96	9.07	8.61
	(3.53)	(3.01)	(2.63)	(2.04)	(3.57)
$PM_{2.5}$, median [IQR], μg/m^3	9.64	12.35	9.24	9.21	7.53
	[7.91–12.21]	[9.73–13.87]	[8.20–11.32]	[7.81–10.23]	[6.67–8.85]
NO_2, mean (SD), μg/m^3	12.59	14.13	11.96	11.29	10.05
	(5.86)	(5.99)	(6.00)	(5.05)	(4.62)
NO_2, median [IQR], μg/m^3	11.79	13.63	10.72	10.60	9.23
	[7.93–16.37]	[9.68–17.90]	[7.42–15.26]	[6.99–15.02]	[6.37–12.90]
Temperature, mean (SD), °C	10.05	8.11	10.41	9.18	11.13
	(6.88)	(7.50)	(6.86)	(6.41)	(7.02)
Temperature, median [IQR], °C	9.74	8.67	10.25	8.13	12.29
	[4.13–16.23]	[1.83–14.60]	[4.45–17.41]	[3.61–16.18]	[4.93–17.70]
Vacation days/month, mean (SD)	7.46	7.19	7.47	7.52	7.72
	(8.22)	(8.03)	(8.43)	(8.07)	(8.33)
Vacation days/month, median [IQR]	6.00	5.00	5.00	7.00	8.00
	[1.00–10.00]	[3.00–9.00]	[2.00–10.00]	[3.00–10.00]	[1.00–11.00]
Lockdown days/month, mean (SD)	1.55	0.00	0.00	9.85	0.00
	(6.51)	(0.00)	(0.00)	(14.11)	(0.00)
Lockdown days/month, median [IQR]	0.00	0.00	0.00	0.00	0.00
	[0.00–0.00]	[0.00–0.00]	[0.00–0.00]	[0.00–28.00]	[0.00–0.00]

Footnote: Values are based on the monthly analytic dataset restricted to working-age adults (18–64 years). Means, standard deviations, medians, and interquartile ranges for continuous variables were weighted by the number of AOK-insured individuals in each aggregated observation unit.

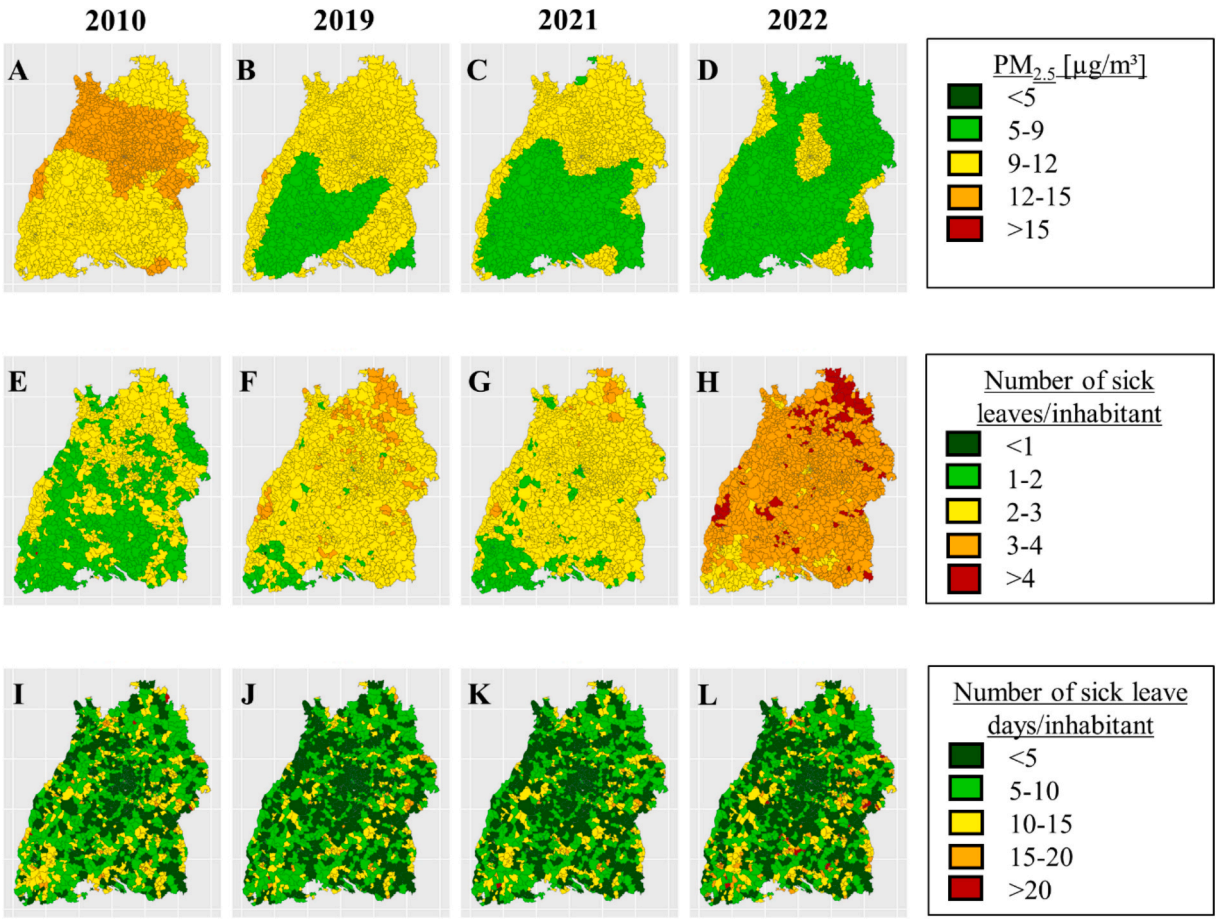


Fig. 1. Spatial resolution of $PM_{2.5}$ exposure, sick leaves, and sick leave days. The figure shows the spatial distribution of $PM_{2.5}$ exposure (A–D), the number of sick-leave episodes per inhabitant (E–H), and the number of sick-leave days per inhabitant (I–L) at the five-digit postal-code level. The selected years represent distinct phases of the study period: 2010 as the first year of observation, 2019 as the last pre-pandemic year, 2021 as a year still characterised by substantial COVID-19-related restrictions, and 2022 as the final study year, when most pandemic-related restrictions had been lifted and electronic sick-leave reporting had become more widely implemented.

areas. Overall, $PM_{2.5}$ showed broader regional patterns rather than pronounced variation between individual five-digit postal-code areas.

Sick-leave episodes showed more pronounced small-area variation across five-digit postal-code areas (Fig. 1E–H). While most postal-code areas recorded approximately 1–2 sick-leave episodes per inhabitant per year in 2010, values were generally higher in the later selected years. A cluster of postal-code areas in the northeast consistently showed higher numbers of sick-leave episodes than other parts of Baden-Württemberg. Sick-leave days also showed substantial small-area variation, but without the pronounced temporal increase observed for sick-leave episodes. Across the selected years, most postal-code areas recorded fewer than 10 sick-leave days per inhabitant, with higher values occurring only in localised areas.

3.4. *Exposure–response relationship between $PM_{2.5}$ and sick-leave days*

In the monthly generalized additive model, several covariates were associated with all-cause sick-leave days. Calendar year showed a positive association with sick leave, corresponding to an average increase of approximately 3.3% per year after adjustment for seasonality, temperature, NO_2 exposure, spatial structure, and the COVID-19 period ($\beta = 0.032$, $p < 0.001$). The COVID-19 period was also associated with higher sick-leave rates ($\beta = 0.035$, $p < 0.001$). Sick-leave rates were higher among men than women ($\beta = 0.196$, $p < 0.001$).

After adjustment for $PM_{2.5}$ and the other covariates, NO_2 showed a small inverse association with sick leave ($\beta = -0.003$ per $\mu g/m^3$, $p < 0.001$), which remained small on the standardised scale (−1.3% per 1 SD increase). Vacation days ($\beta = -0.010$, −7.9%, $p < 0.001$) and lockdown days ($\beta = -0.017$, −9.9%, $p < 0.001$) were also associated with lower sick-leave rates, corresponding to standardised relative changes of −7.9% and −9.9% per 1-SD increase, respectively. For comparability across continuous linear covariates, additional SD-standardised effect estimates indicated a substantially larger association for calendar year (+12.8% per 1 SD) than for NO_2. The exposure–response relationship between $PM_{2.5}$ and sick leave was modelled using a penalised spline and showed a non-linear association (effective degrees of freedom [EDF] = 8.82, $F = 304.9$, $p < 0.001$). Temperature also showed a non-linear association with sick leave (EDF = 8.89, $F = 705.2$, $p < 0.001$) (Table 2, Fig. 3). Spatial heterogeneity was captured by the postal-code-based Markov random field term (EDF = 9.00, $F = 4222.1$, $p < 0.001$). Overall, the model explained 55.1% of the deviance in monthly all-cause sick leave, indicating good agreement between the model and the observed data.

The exposure–response relationship between ambient $PM_{2.5}$ concentrations and all-cause sick leave showed a non-linear pattern (Fig. 3). Modelling $PM_{2.5}$ using a penalised spline indicated that the association was not adequately represented by a simple linear specification (EDF = 8.82, $F = 304.9$, $p < 0.001$).

In the primary model, sick leave increased steeply at lower $PM_{2.5}$ concentrations, particularly between 5 and 10 $\mu g/m^3$. Between approximately 10 and 15 $\mu g/m^3$, the curve showed an apparent plateau-like segment, with little additional increase in sick leave despite

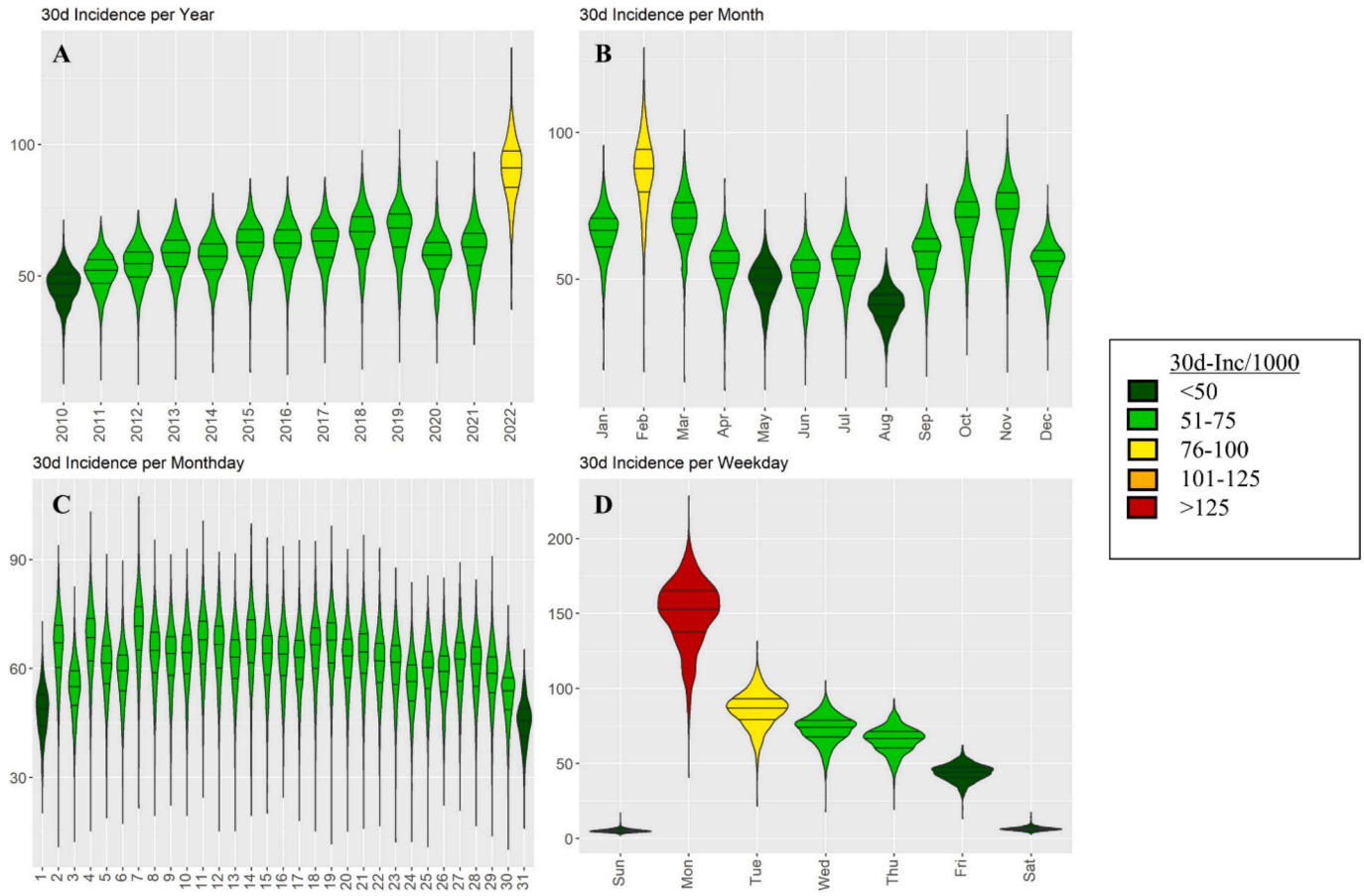


Fig. 2. Temporal resolution and seasonality of sick leaves. The figure shows 30-day sick-leave incidence per 1,000 insured persons across different temporal resolutions: (A) by year, (B) by calendar month (aggregated across years), (C) by day of month (aggregated across years), and (D) by weekday (aggregated across years).

Table 2
Associations between $PM_{2.5}$ exposure and all-cause sick leave days based on a generalized additive model and monthly aggregations.

Variable / Term	Estimate (β)	SE	t / F	p-value
Parametric effects				
Intercept	−66.95	0.31000	−214.97	<0.001
Year	0.0321	0.00015	207.34	<0.001
Male (vs. female)	0.1960	0.00073	266.63	<0.001
COVID period (vs. non-COVID period)	0.0349	0.00143	24.37	<0.001
NO_2 (μg/m^3)	−0.0025	0.00015	−16.49	<0.001
Vacation days	−0.0100	0.00015	−66.64	<0.001
Lockdown days	−0.0167	0.00007	−237.96	<0.001
Smooth terms	**EDF**		**F**	
$PM_{2.5}$ (μg/m^3)	8.82		304.9	<0.001
Temperature (°C)	8.89		705.2	<0.001
Spatial effect (postal code, MRF)	9.00		4222.1	<0.001
Model performance				
Deviance explained	55.1%			

Footnote: Model was adjusted for long-term trend (calendar year), seasonality (monthly), temperature, spatial effects (postal-code-based MRF), sex, COVID period, NO_2, vacation days, and lockdown days. Seasonality was modelled using orthogonal polynomial contrasts of calendar month.

increasing $PM_{2.5}$ concentrations. Above approximately 15 μg/m^3, sick leave increased again before the slope appeared to diminish toward the upper end of the displayed exposure range. Overall, the fitted curve was inconsistent with a simple linear or single-threshold relationship; however, the precise shape of the exposure–response function was further examined in sensitivity analyses.

3.5. Model-based $PM_{2.5}$ exposure contrasts derived from the fitted exposure–response model

Because $PM_{2.5}$ was modelled using a penalised smooth term, no single global coefficient for the $PM_{2.5}$ association can be directly interpreted.

Table 3 shows the resulting model-based $PM_{2.5}$ exposure contrasts derived from average adjusted predictions. Increasing $PM_{2.5}$ from 5 to 10 μg/m^3 was associated with a 9.56% higher predicted sick-leave rate (95% CI 9.09 to 10.00). In contrast, the contrast between 10 and 15 μg/m^3 indicated little additional change (+0.04%, 95% CI − 0.30 to 0.38). At higher concentrations, sick leave increased again, with a 4.92% higher predicted sick-leave rate for 20 compared with 15 μg/m^3 (95% CI 4.34 to 5.49). Overall, $PM_{2.5}$ at 20 μg/m^3 was associated with a 15.00% higher predicted sick-leave rate compared with the WHO guideline concentration of 5 μg/m^3 (95% CI 14.20 to 15.80).

3.6. Sensitivity and subgroup analyses

Sensitivity analyses using alternative temporal aggregations supported the presence of a non-linear association between $PM_{2.5}$ exposure and sick leave. The $PM_{2.5}$ smooth remained highly significant in the primary monthly model (EDF = 8.82, F = 304.9, $p < 0.001$), as well as in the quarterly model (EDF = 8.33, F = 204.2, $p < 0.001$, **Supplementary Table e2**) and the weekly model (EDF = 7.61, F = 180.0, $p < 0.001$, **Supplementary Table e3**). In additional sensitivity analyses of temporal adjustment, the monthly model was refitted with calendar year

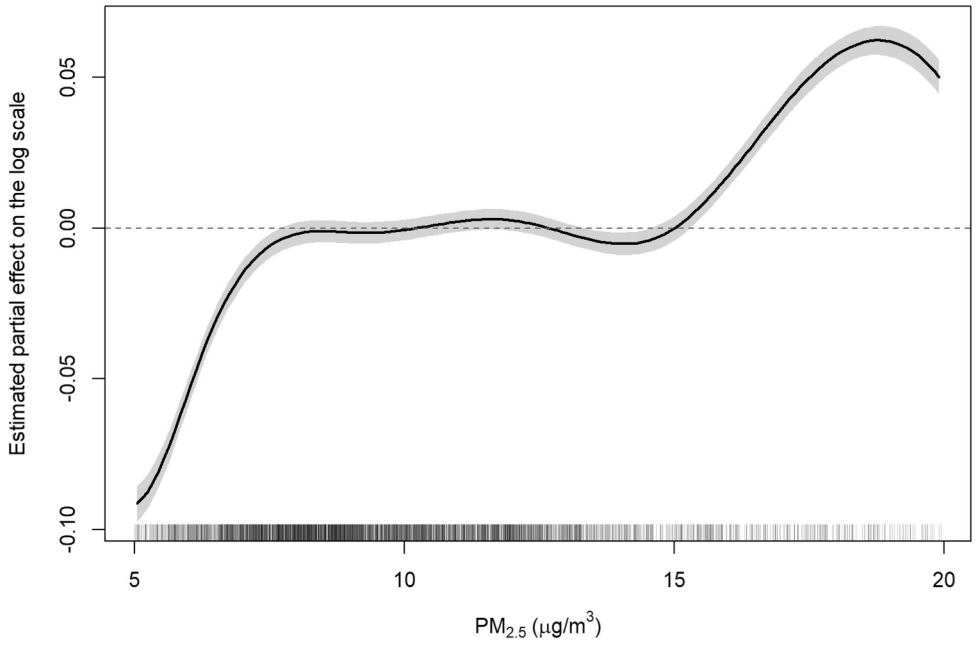


Fig. 3. Estimated exposure–response relationship between $PM_{2.5}$ exposure and sick leave days. The figure shows the estimated exposure–response relationship between ambient $PM_{2.5}$ concentration and sick-leave days from the monthly generalized additive model. To facilitate interpretation and reduce the visual influence of sparse extreme values, the curve is displayed for the range from 5 to 20 µg/m^3, which closely corresponds to the central 95% of the observed $PM_{2.5}$ distribution (2.5th percentile: 5.41 µg/m^3; 97.5th percentile: 19.50 µg/m^3). This restriction was applied for graphical presentation only and did not affect model estimation or statistical inference. The rug plot indicates the distribution of observed $PM_{2.5}$ values within the displayed range. Shaded areas indicate 95% simultaneous confidence intervals.

Table 3
Model-based $PM_{2.5}$ exposure contrasts and percentage changes in predicted monthly all-cause sick-leave rates.

$PM_{2.5}$ exposure range	Change in sick leave days (%)	95% CI
5 µg/m^3 to 10 µg/m^3	+9.56	9.09 to 10.00
10 µg/m^3 to 15 µg/m^3	+0.04	−0.30 to 0.38
15 µg/m^3 to 20 µg/m^3	+4.92	4.34 to 5.49
5 µg/m^3 to 20 µg/m^3	+15.00	14.20 to 15.80

Footnote: Exposure contrasts were derived from average adjusted predictions of the fitted generalized additive model on the response scale at selected $PM_{2.5}$ concentrations. $PM_{2.5}$ was set to predefined values while all other covariates were kept at their observed values, and predictions were averaged across the study population. Values represent percentage changes in predicted sick-leave rates with 95% confidence intervals.

modelled as a smooth term, with time since the start of the COVID-19 pandemic added to the model, with time since pandemic start used instead of the binary COVID-19 indicator, and with a calendar year × COVID-19 interaction. Across these alternative temporal specifications, the $PM_{2.5}$ smooth remained highly significant (all $p < 0.001$), with EDF values ranging from 7.21 to 8.82 (Supplementary Table e4).

When the analysis was restricted to the pre-pandemic period from 2010 to 2019, the $PM_{2.5}$ association remained non-linear and highly significant (EDF = 8.86, F = 130.5, $p < 0.001$). However, the estimated contrasts were attenuated compared with the primary analysis: predicted sick-leave rates increased by 2.62% (95% CI 1.99 to 3.26) from 5 to 10 µg/m^3, by 1.70% (95% CI 1.37 to 2.02) from 10 to 15 µg/m^3, and by 2.01% (95% CI 1.47 to 2.55) from 15 to 20 µg/m^3, corresponding to an overall increase of 6.47% (95% CI 5.55 to 7.41) between 5 and 20 µg/m^3.

Excluding NO_2 from the primary model yielded a broadly similar non-linear pattern. The $PM_{2.5}$ smooth remained highly significant (EDF = 8.82, F = 274.5, $p < 0.001$), with estimated changes of + 8.53% (95% CI 8.08 to 9.04), −0.79% (95% CI − 1.09 to − 0.46), and + 4.29% (95% CI 3.74 to 4.82) for the 5–10, 10–15, and 15–20 µg/m^3 contrasts, respectively. The corresponding 5–20 µg/m^3 contrast was + 12.30% (95% CI 11.60 to 13.00).

Exploratory sex-specific analyses showed significant non-linear $PM_{2.5}$ associations in both women (EDF = 8.67, F = 210.0, $p < 0.001$) and men (EDF = 8.68, F = 172.6, $p < 0.001$). The overall 5–20 µg/m^3 contrast was + 16.10% (95% CI 15.10 to 17.20) in women and + 13.80% (95% CI 12.70 to 14.80) in men. Differences between the sex-specific exposure contrasts were statistically significant across the examined concentration intervals, indicating some heterogeneity in the shape of the exposure–response relationship; however, these subgroup findings should be considered exploratory (Supplementary Table e5).

3.7. Model-based sick-leave burden and associated productivity losses

Based on the monthly generalized additive model, $PM_{2.5}$ exposure above the counterfactual concentration of 5 µg/m^3 was associated with 105 model-attributable excess sick-leave days per 1,000 working-age inhabitants per year. Applied to the working-age population of Baden-Württemberg (6.88 million), this corresponded to approximately 722,400 excess sick-leave days per year. Using the estimated average daily labour cost of €292.96, the corresponding annual productivity losses were approximately €212 million within the study region.

In an additional scenario-based extrapolation to the German working-age population of 50,597,024 individuals, assuming that the burden rate estimated for Baden-Württemberg was applicable to Germany as a whole, this corresponded to approximately 5.31 million excess sick-leave days per year and €1.56 billion in annual productivity losses.

4. Discussion

4.1. Key findings

To our knowledge, this study is among the first large-scale analyses to examine the association between longer-term regional $PM_{2.5}$ exposure and all-cause sickness absence using routinely collected health-

insurance data over an extended observation period. Previous studies have predominantly focused on short-term exposure and acute triggering effects, whereas our analysis addresses the complementary question of whether persistent regional exposure patterns are associated with the overall burden of sick leave. In addition, the study combines a flexible non-linear exposure–response analysis with an estimation of the associated population-level and economic burden.

The main finding was a non-linear association between monthly $PM_{2.5}$ exposure and all-cause sick-leave days. In the primary model, higher predicted sick-leave rates were observed already at relatively low concentrations, with a comparatively flat mid-exposure segment and a renewed increase at higher concentrations. The overall non-linear association was supported across alternative analyses, although the magnitude and precise shape of the exposure–response function varied with temporal coverage and covariate adjustment. $PM_{2.5}$ concentrations above the WHO annual guideline of 5 $\mu g/m^3$ were associated with a substantial model-attributable burden of sickness absence, corresponding to approximately 722,400 excess sick-leave days and €212 million in annual productivity losses in Baden-Württemberg. A scenario-based extrapolation to the German working-age population yielded approximately 5.31 million excess sick-leave days and €1.56 billion in annual productivity losses. These findings extend the existing literature by linking longer-term regional $PM_{2.5}$ exposure not only to sickness absence but also to its potential population-level and economic implications.

4.2. Spatial patterns and temporal dynamics of sick leave

The spatial distribution of $PM_{2.5}$ exposure showed elevated concentrations in central Baden-Württemberg and along the western border, particularly in 2022. Similar spatial patterns have previously been reported for Baden-Württemberg for the period 2010–2018 (Rittweger et al., 2022). Higher concentrations in the central part of the state are likely related to the urban and densely populated area around Stuttgart, whereas elevated exposure along the western border may reflect the Rhine corridor, which is characterised by shipping activity and major transport routes on both sides of the river (Hoffmann et al., 2024; Rittweger et al., 2022).

Sick-leave episodes increased over time, with a particularly marked rise between 2021 and 2022. This increase likely reflects a combination of epidemiological and administrative factors. First, the spread of the Omicron variant led to a strong increase in COVID-19 incidence during this period (Hoffmann et al., 2025). Second, the introduction of electronic sick-leave reporting in Germany in 2022 may have improved the capture of short-term sick-leave episodes that may previously have been underreported. This interpretation is supported by the observation that the number of sick-leave episodes increased, whereas sick-leave days per inhabitant did not increase to the same extent. The spatial distribution of sick-leave episodes in 2022 also resembled previously described regional patterns of COVID-19 incidence, suggesting that pandemic dynamics contributed to the observed increase (Hoffmann et al., 2025).

Temporal analyses further showed pronounced seasonal, within-month, and weekday patterns. Sick-leave incidence was highest in winter, with a peak in February, and lowest in summer. This pattern is consistent with seasonal variation in respiratory infections and with previous evidence showing that lower temperatures are associated with higher incidence of COVID-19 and influenza (Hoffmann et al., 2024; Rittweger et al., 2022). The lower incidence observed at the beginning and end of months may partly reflect calendar effects, including public holidays, Christmas holidays, and the fact that not all months have the same number of days. Weekday patterns showed a clear peak on Mondays, which may reflect delayed presentation for illnesses that began during the weekend. Conversely, Fridays showed the lowest incidence among working days, possibly because some individuals postpone formal sick-leave reporting and use the weekend for recovery, as suggested previously (Kriit et al., 2024).

4.3. Reducing $PM_{2.5}$ exposure as a public health and economic measure

Previous studies on air pollution and sickness absence have primarily examined short-term exposure, whereas the present study addresses a complementary longer-term exposure perspective. Mahakalkar et al. (2026) used daily exposure data and a case-crossover design in Baden-Württemberg to investigate acute effects of short-term air-pollution fluctuations on sick leave, while Kriit et al. (2024) similarly examined short-term $PM_{2.5}$ exposure in Stockholm and reported an 8.5% increase in the odds of initiating a sick-leave episode per 10 $\mu g/m^3$ increase in exposure 2–4 days earlier. Earlier work from Oslo also suggested an association between short-term particulate pollution and sickness absence (Hansen and Selte, 2000). In contrast, our analysis used monthly $PM_{2.5}$ concentrations repeatedly over a 13-year period and modelled the total number of all-cause sick-leave days rather than the acute onset of individual sick-leave episodes. These differences in exposure window, outcome definition, study design, and spatial scale limit direct numerical comparison of effect estimates. Nevertheless, the direction of association is consistent across studies, suggesting that particulate air pollution may be relevant both as a short-term trigger of sickness absence and as a correlate of the longer-term regional burden of sick leave.

Our findings also extend previous work by demonstrating a non-linear exposure–response pattern rather than assuming a constant association across the exposure range. In the primary analysis, predicted sick leave increased markedly at lower $PM_{2.5}$ concentrations, showed a comparatively flat segment between approximately 10 and 15 $\mu g/m^3$, and increased again at higher concentrations. However, sensitivity analyses showed that the precise shape and magnitude of the exposure–response function varied across model specifications, particularly when the analysis was restricted to the pre-pandemic period. Thus, the overall evidence supports a non-linear association, whereas the apparent mid-range plateau should not be interpreted as a stable threshold or saturation point. This is consistent with evidence from other $PM_{2.5}$-related health outcomes showing that concentration–response relationships may be non-linear and that adverse associations can occur even at relatively low concentrations.

The small inverse association observed for NO_2 should be interpreted cautiously and should not be considered evidence of a protective effect. NO_2 and $PM_{2.5}$ represent correlated components of the ambient air-pollution mixture, and estimates from multipollutant models may be sensitive to collinearity, differences in spatial and temporal variation, and adjustment for shared sources and covariates. Previous studies have shown that effect estimates for NO_2 can be substantially attenuated or altered after adjustment for $PM_{2.5}$ and that correlated exposures may even produce sign changes in jointly adjusted regression coefficients (Basagaña and Barrera-Gómez, 2022; Chen et al., 2024; Ji et al., 2022). Accordingly, the inverse NO_2 coefficient in the present model may reflect statistical adjustment within a correlated pollutant mixture, residual spatial or temporal confounding, or differences in the exposure patterns captured by NO_2 and $PM_{2.5}$ rather than a biologically protective association. The primary exposure of interest was $PM_{2.5}$, and the NO_2 estimate should therefore be regarded mainly as an adjusted co-pollutant coefficient rather than as an independently interpretable exposure association.

Together, these findings suggest that $PM_{2.5}$ exposure is not only associated with clinical morbidity, but also with measurable impairment in daily functioning and labour market participation. This broader economic relevance becomes clearer when compared with other established determinants of sickness absence. Smoking, obesity, and depression have all been linked to increased absenteeism and substantial productivity losses (Cawley et al., 2007; Cocker et al., 2014; Troelstra et al., 2020). Although the mechanisms and exposure patterns differ, these comparisons indicate that $PM_{2.5}$ should be considered alongside other major determinants of work absence. Unlike behavioural risk factors, however, ambient air pollution affects entire populations and is

only minimally modifiable at the individual level. This strengthens the case for structural prevention through air-quality policy rather than relying solely on individual behavioural change.

Our counterfactual analysis quantifies the model-based difference in sickness absence associated with a scenario in which $PM_{2.5}$ concentrations were set to the WHO annual guideline of 5 $\mu g/m^3$. Compared with the observed exposure distribution, this scenario corresponded to approximately 105 fewer predicted sick-leave days per 1,000 working-age inhabitants per year. Applied to Baden-Württemberg, this was equivalent to approximately 722,400 fewer predicted sick-leave days and about €212 million in annual productivity losses. In the additional scenario-based extrapolation to Germany, the corresponding estimates were approximately 5.31 million fewer predicted sick-leave days and €1.56 billion in annual productivity losses per year. These estimates should be interpreted as model-based counterfactual scenarios rather than as causal forecasts of the effects of a specific air-quality intervention. Nevertheless, lower population-level $PM_{2.5}$ exposure could be associated with both public health and economic benefits, which is particularly relevant in ageing societies with increasing pressure on health, social insurance, and labour-market systems. Reducing $PM_{2.5}$ exposure may therefore yield a double dividend: improved population health and lower productivity losses. This is particularly relevant in ageing societies, where shrinking labour supply, increasing care needs, and growing pressure on health and social insurance systems make the prevention of avoidable sickness absence an important public health and economic priority.

4.4. Potential pathways and future directions

The association between $PM_{2.5}$ exposure and sickness absence can be interpreted within a broader exposome framework, in which environmental exposures interact with biological and contextual factors across the life course (Vineis and Barouki, 2022). At the biological level, $PM_{2.5}$ exposure can promote oxidative stress, systemic inflammation, autonomic imbalance, endothelial dysfunction, and respiratory and cardiovascular impairment, providing plausible pathways through which air pollution may reduce functional capacity and increase the likelihood of sickness absence (Anderson et al., 2012; Aretz et al., 2021; Krittanawong et al., 2023). Evidence linking longer-term $PM_{2.5}$ exposure to impaired cognitive functioning and inflammatory processes further supports systemic effects that may be relevant for work ability (Aretz et al., 2024).

The observed non-linear exposure–response pattern suggests that the association may vary across the exposure distribution. Previous research on other $PM_{2.5}$-related health outcomes has similarly indicated adverse associations at relatively low concentrations and concentration–response functions that are not necessarily linear (Chen and Hoek, 2020; Liu et al., 2019; Masselot et al., 2022). Differences in particle composition and source profiles may additionally contribute to heterogeneity in health effects across locations and exposure levels (Sun et al., 2024). In the present study, sensitivity analyses supported the overall non-linear association but showed that its precise shape was not fully stable across model specifications. In particular, restriction to the pre-pandemic period yielded a more evenly distributed increase across the exposure range, whereas omission of NO_2 adjustment broadly preserved the pattern observed in the primary model. The apparent plateau between approximately 10 and 15 $\mu g/m^3$ should therefore not be interpreted as evidence of a biological threshold or saturation effect; it may partly reflect the temporal distribution of exposure, residual confounding, or differences in data support across the exposure range.

Future studies should further investigate potential effect modification by individual characteristics beyond sex, including age, occupation, socioeconomic factors, and cause of sickness absence, and should examine the robustness of the observed exposure–response shape using alternative high-resolution exposure assessments and information on $PM_{2.5}$ source composition.

4.5. Strengths and limitations

This study used a large routine health insurance dataset covering approximately 4.5 million AOK policyholders in Baden-Württemberg over 13 years, allowing analyses of sick leave across urban and rural areas. Administrative sick-leave records reduced recall bias and provided an objective, policy-relevant outcome. $PM_{2.5}$ exposure was assessed consistently using CAMS reanalysis data aggregated to five-digit postal-code areas. Generalized additive models fitted with the bam function from the *mgcv* package in R allowed flexible modelling of non-linear exposure–response relationships while accounting for population size, temporal patterns, and spatial heterogeneity — even with large datasets and "standard" computing power. The overall non-linear $PM_{2.5}$ association was supported across alternative temporal aggregations and specifications, restriction to the pre-pandemic period, and omission of NO_2 adjustment, although the magnitude and precise shape of the exposure–response function varied across sensitivity analyses.

Because both exposure and outcome information were analysed at the aggregated postal-code level, associations observed at the area level cannot necessarily be interpreted as individual-level associations. This creates the possibility of ecological bias. In addition, age and diagnosis-specific causes of sickness absence were not available at the required resolution in the final aggregated analytical dataset, and individual-level information on occupation, smoking, socioeconomic position, comorbidities, workplace characteristics, and other behavioural or social determinants was not available. Residual confounding by these factors therefore cannot be excluded.

Exposure was assigned according to residential postal-code area and therefore represents an area-level ambient exposure metric rather than individual personal exposure. Workplace exposure, commuting-related exposure, time spent away from home, indoor air pollution, and individual activity patterns were not captured, which may have introduced exposure misclassification, particularly among working-age adults. In addition, the relatively coarse native spatial resolution of the CAMS air quality reanalysis (approximately 10 × 10 km) may not fully capture local $PM_{2.5}$ gradients, particularly in urban areas or near major emission sources (Handschuh et al., 2026; Mahakalkar et al., 2026). Although bilinear resampling improved the spatial allocation of concentrations to irregular postal-code boundaries, it did not increase the underlying spatial information of the original CAMS data and could not recover sub-grid variability or local pollution hotspots. This may have attenuated spatial contrasts between neighbouring postal-code areas; if exposure misclassification was predominantly non-differential with respect to sick leave, associations may have been biased towards the null, although the direction and magnitude of bias cannot be determined with certainty. Commuting-related exposure may also contribute to misclassification; Gilardi et al. (2024) estimated that ignoring commuting can modestly underestimate population exposure to $PM_{2.5}$ above the WHO guideline, particularly in urban areas. Accordingly, the findings should be interpreted as area-level associations between regional monthly $PM_{2.5}$ exposure and aggregated sickness absence rather than as direct causal effects of individual exposure.

Sick leave may also be influenced by occupational, social, and administrative factors, including telework, reduced working hours, insurance status, and the introduction of electronic sick-leave reporting in 2022. In addition, the study population was restricted to Baden-Württemberg, and both population characteristics and ambient $PM_{2.5}$ exposure distributions vary across Germany. The national health-economic estimates should therefore be interpreted as scenario-based extrapolations rather than direct estimates for Germany. They assume that the model-attributable sick-leave burden estimated in Baden-Württemberg is transferable to the German working-age population as a whole. This assumption may not fully hold because regional differences in population structure, labour-market characteristics, sickness-certification practices, healthcare utilisation, insurance composition, and air-pollution exposure may affect the absolute burden. We therefore

additionally report the corresponding estimate for Baden-Württemberg, which more directly reflects the population from which the underlying association was derived.

In addition, because observations at the tails of the $PM_{2.5}$ distribution were sparse and associated with greater uncertainty, interpretation was restricted to the central exposure range (5–20 $\mu g/m^3$), which closely corresponded to the central 95% of the observed distribution. Finally, the health-economic estimates did not include presenteeism, unpaid work, healthcare costs, or broader societal consequences, suggesting that the total economic burden may be higher than estimated.

5. Conclusion

$PM_{2.5}$ exposure was associated with a relevant model-attributable burden of sick leave and showed a non-linear exposure–response relationship. Although the magnitude and precise shape of the association varied with temporal coverage and covariate adjustment, higher $PM_{2.5}$ exposure was consistently associated with greater sickness absence over the overall exposure range. These findings highlight ambient $PM_{2.5}$ as a potentially important population-level correlate of work absence and associated productivity losses, with lower long-term $PM_{2.5}$ exposure potentially associated with lower sickness absence and economic burden.

Ethical approval

The study was approved by the Ethical Committee of the Medical Council (Landesärztekammer Nordrhein) within the VARIAQ study (lfd Nr 2020092).

Consent for publication

Not applicable.

CRediT authorship contribution statement

Benjamin Aretz: Writing – original draft, Visualization, Methodology, Investigation, Formal analysis, Data curation, Conceptualization. **Jonas Böcker:** Writing – review & editing, Visualization, Investigation, Data curation. **Michael Arz:** Writing – review & editing, Investigation. **Lorenza Gilardi:** Writing – review & editing, Resources, Methodology. **Matthias Schmid:** Writing – review & editing, Supervision, Methodology. **Michael Bittner:** Writing – review & editing, Supervision, Resources, Methodology, Conceptualization. **Jörn Rittweger:** Supervision, Resources, Methodology, Conceptualization.

Funding

Open Access funding enabled and organized by Projekt DEAL. This study was performed with internal funding of DLR and AOK Baden-Württemberg.

Declaration of competing interest

The authors declare that they have no known competing financial interests or personal relationships that could have appeared to influence the work reported in this paper.

Acknowledgements

This research was initiated and intellectually guided by Jörn Rittweger. We dedicate this work to his memory in recognition of his pivotal role in shaping the study, his passion for the topic of environmental health stressor, and last but not least his enduring scientific legacy.

Appendix A. Supplementary data

Supplementary data to this article can be found online at https://doi.org/10.1016/j.envint.2026.110586.

Data availability

Data will be made available on request.

The data that support the findings of this study are available on request from JB. The data are not publicly available due to the high standards of data protection for health data.

References

Anderson, Jonathan O., Thundiyil, Josef G., Stolbach, Andrew, 2012. Clearing the air: a review of the effects of particulate matter air pollution on human health. *Journal of Medical Toxicology : Official Journal of the American College of Medical Toxicology* 8 (2), S. 166–S.175. https://doi.org/10.1007/s13181-011-0203-1.

Aretz, Benjamin, Doblhammer, Gabriele, Heneka, Michael T., 2024. The role of leukocytes in cognitive impairment due to long-term exposure to fine particulate matter: A large population-based mediation analysis. *Alzheimer's & Dementia : The Journal of the Alzheimer's Association* 20 (12), S. 8715–S. 8727. https://doi.org/10.1002/alz.14320.

Aretz, B., Janssen, F., Vonk, J.M., Heneka, M.T., Boezen, H.M., Doblhammer, G., 2021. Long-term exposure to fine particulate matter, lung function and cognitive performance: a prospective dutch cohort study on the underlying routes. Environ. Res. 201. https://doi.org/10.1016/j.envres.2021.111533. S. 111533.

Bang Christensen, Karl, Lund, Thomas, Labriola, Merete, Villadsen, Ebbe, Bültmann, Ute, 2007. The fraction of long-term sickness absence attributable to work environmental factors: prospective results from the danish work environment cohort study. Occup. Environ. Med. 64 (7), S487–S489. https://doi.org/10.1136/oem.2006.028563.

Basagaña, Xavier, Barrera-Gómez, Jose, 2022. Reflection on modern methods: visualizing the effects of collinearity in distributed lag models. Int. J. Epidemiol. 51 (1), S334–S344. https://doi.org/10.1093/ije/dyab179.

Bauer, A., Weber, E., 2021. COVID-19: how much unemployment was caused by the shutdown in Germany? Appl. Econ. Lett. 28 (12), 1053–1058. https://doi.org/10.1080/13504851.2020.1789544.

Blomgren, J., 2015. Regional differences in sickness absence in Finland: individual and area effects in 2010–2011. Eur. J. Pub. Health 25 (suppl_3). https://doi.org/10.1093/eurpub/ckv167.050.

Brocke, Stephanie A., Smyth, Timothy, Dang, Hong, Speen, Adam, Kim, Yong Ho, Christianson, Cara, et al., 2025. Seasonal PM2.5 exposures induce differential responses to influenza A virus infection in primary human airway epithelial cells. Part. Fibre Toxicol. 22 (1), S28. https://doi.org/10.1186/s12989-025-00643-8.

Cawley, John, Rizzo, John A., Haas, Kara, 2007. Occupation-specific absenteeism costs associated with obesity and morbid obesity. J. Occup. Environ. Med. 49 (12), S1317–S1324. https://doi.org/10.1097/JOM.0b013e31815b56a0.

Chambers, John M. (Hg.) (1997): Statistical models in S. Reprint. London: Chapman & Hall (Chapman & Hall computer science series).

Chen, J., Hoek, G., 2020. Long-term exposure to PM and all-cause and cause-specific mortality: a systematic review and meta-analysis. Environ. Int. 143. https://doi.org/10.1016/j.envint.2020.105974. S. 105974.

Chen, Xuan, Gehring, Ulrike, Dyer, Georgia M.C., Khomenko, Sasha, Hoogh, Kees de, Tonne, Cathryn, et al., 2024. Single- and two-pollutant concentration-response functions for PM2.5 and NO2 for quantifying mortality burden in health impact assessments. Environ. Res. 263 (Pt3). https://doi.org/10.1016/j.envres.2024.120215. S. 120215.

Cocker, F., Nicholson, J.M., Graves, N., Oldenburg, B., Palmer, A.J., Martin, A., et al., 2014. Depression in working adults: comparing the costs and health outcomes of working when ill. In: Plos One 9 (9), e105430. https://doi.org/10.1371/journal.pone.0105430.

Copernicus Atmosphere Monitoring Service (2021): CAMS European air quality reanalyses.

Copernicus Climate Change Service (2019): ERA5-Land hourly data from 1950 to present.

Destatis Statistisches Bundesamt (2025c): Staff on sick leave. Quality of employment. Federal Statistical Office. Wiesbaden. Online verfügbar unter https://www.destatis.de/EN/Themes/Labour/Labour-Market/Quality-Employment/Dimension2/2_3_StaffSickLeave.html.

Destatis Statistisches Bundesamt (2024): Despite the leap year: 0.6 fewer workdays in 2024 compared to the previous year. Online verfügbar unter https://www.destatis.de/DE/Presse/Pressemitteilungen/Zahl-der-Woche/2024/PD24_06_p002.html.

Destatis Statistisches Bundesamt (2026): Population: Germany, reference date, age. Code: 12411-0005. Online verfügbar unter https://genesis.destatis.de/datenbank/online/statistic/12411/table/12411-0005.

Gabbay, Mark; Taylor, Lorraine; Sheppard, Linda; Hillage, Jim; Bambra, Clare; Ford, Fiona et al. (2011): NICE guidance on long-term sickness and incapacity. In: *The British journal of general practice : the journal of the Royal College of General Practitioners* 61 (584), e118-24. DOI: 10.3399/bjgp11X561221.

Gilardi, Lorenza; Erbertseder, Thilo; Baier, Frank; Paeth, Heiko; Ullmann, Tobias; Taubenböck, Hannes (2024): The Influence of Commuting on Population Exposure to Air Pollution: Toward Global Application With a Proxy on the Degree of

Urbanization. In: *IEEE J. Sel. Top. Appl. Earth Observations Remote Sensing* 17, S. 12720–12730. DOI: 10.1109/JSTARS.2024.3420155.
Hahad, O., Lelieveld, J., Al-Kindi, S., Schmitt, V.H., Hobohm, L., Keller, K., et al., 2025. Burden of disease in Germany attributed to ambient particulate matter pollution. Herz 50 (1), 42–50. https://doi.org/10.1007/s00059-024-05269-8.
Handschuh, Jana; Baier, Frank; Molina García, Víctor; Friedl, Peter; Loyola, Diego (2026): TROPOMI-Based PM2.5 Estimates and Their Evaluation During a High-Pollution Event in Germany. In: *Remote Sensing* 18 (4), S. 562. DOI: 10.3390/rs18040562.
Hansen, A.C., Selte, H.K., 2000. Air pollution and sick-leaves. Environ. Resour. Econ. 16 (1), 31–50. https://doi.org/10.1023/A:1008318004154.
Hoffmann, L., Gilardi, L., Antoni, T., Baltruweit, M., Bittner, M., Breitner, S., et al., 2025. Modulation of COVID-19 incidence by environmental stressors is variant between pre-Omicron and Omicron periods. Sci. Rep. 15 (1). https://doi.org/10.1038/s41598-025-13521-2. S. 27636.
Hoffmann, L., Gilardi, L., Schmitz, M.-T., Erbertseder, T., Bittner, M., Wüst, S., et al., 2024. Investigating the spatiotemporal associations between meteorological conditions and air pollution in the federal state Baden-Württemberg (Germany). Sci. Rep. 14 (1). https://doi.org/10.1038/s41598-024-56513-4. S. 5997.
Hsiao, Ta-Chih; Cheng, Po-Ching; Chi, Kai Hsien; Wang, Hung-Yang; Pan, Shih-Yu; Kao, Ching et al. (2022): Interactions of chemical components in ambient PM2.5 with influenza viruses, *Journal of Hazardous Materials.* 423(PtB) S127243 Doi: 10.1016/j.jhazmat.2021.127243.
IAB Institute for Employment Research (2023): IAB Data Base on Coronavirus Containment Measures, Version 5 (corrected 9 March 2023). Institute for Employment Research. Nürnberg. Online verfügbar unter https://iab.de/en/daten/iab-data-base-on-coronavirus-containment-measures/.
Ji, John S., Liu, Linxin, Zhang, Junfeng jim, Kan, Haidong, Zhao, Bin, Burkart, Katrin G., Zeng, Yi, 2022. NO2 and PM2.5 air pollution co-exposure and temperature effect modification on pre-mature mortality in advanced age: a longitudinal cohort study in China. Environ. HealthA Global Access Science Source. 21 (1), S97. https://doi.org/10.1186/s12940-022-00901-8.
KMK Standing Conference of the Ministers of Education and Cultural Affairs of the Länder in the Federal Republic of Germany (2026): Holiday regulations [Ferienregelung]. Berlin/Bonn. Online verfügbar unter https://www.kmk.org/service/ferienregelung.html.
Kriit, H.K., Forsberg, Bertil, Nilsson, Johan Sommar, 2024. Increase in sick leave episodes from short-term fine particulate matter exposure: a case-crossover study in Stockholm, Sweden. Environ. Res. 244. https://doi.org/10.1016/j.envres.2023.117950. S. 117950.
Krittanawong, Chayakrit; Qadeer, Yusuf Kamran; Hayes, Richard B.; Wang, Zhen; Thurston, George D.; Virani, Salim; Lavie, Carl J. (2023): PM2.5 and cardiovascular diseases: State-of-the-Art review. In: *International journal of cardiology. Cardiovascular risk and prevention* 19, S. 200217. DOI: 10.1016/j.ijcrp.2023.200217.
Li, N., Ma, J., Ji, K., Wang, L., 2022. Association of PM2.5 and PM10 with acute exacerbation of chronic obstructive pulmonary disease at lag0 to lag7: A systematic review and meta-analysis. COPD 19 (1), 243–254. https://doi.org/10.1080/15412555.2022.2070062.
Lin, M.-W., Lin, C.-H., Chang, J.-R., Chiang, H.-H., Wu, T.-H., Lin, C.-S., 2025. The influence of PM2.5 exposure on SARS-CoV-2 infection via modulating the expression of angiotensin converting enzyme II. J. Hazard. Mater. 485. https://doi.org/10.1016/j.jhazmat.2024.136887. S. 136887.
Liu, Cong, Chen, Renjie, Sera, Francesco, Vicedo-Cabrera, Ana M., Guo, Yuming, Tong, Shilu, et al., 2019. Ambient particulate air pollution and daily mortality in 652 cities. The New England Journal of Medicine. 381 (8), S705–S715. https://doi.org/10.1056/NEJMoa1817364.
Jason, Ma, Chiu, Ya-Fang, Kao, Chih-Chen, Chuang, Chun-Ning, Chen, Chi-Yuan, Lai, Chih-Ho, Kuo, Ming-Ling, 2024. Fine particulate matter manipulates immune response to exacerbate microbial pathogenesis in the respiratory tract. European Respiratory Review : An Official Journal of the European Respiratory Society. 33 (173). https://doi.org/10.1183/16000617.0259-2023.
Mahakalkar, Amruta Umakant, Gianquintieri, Lorenzo, Gilardi, Lorenza, Erbertseder, Thilo, Baier, Frank, Dally, Simon, et al., 2026. Short-term exposure to air pollution and acute health effects in a low-pollution region Baden-Wurttemberg, Germany. Environ. Sci. Eur. 38 (1). https://doi.org/10.1186/s12302-026-01406-8.
Marécal, V., Peuch, V.-H., Andersson, C., Andersson, S., Arteta, J., Beekmann, M., et al., 2015. A regional air quality forecasting system over Europe: the MACC-II daily ensemble production. In: Geosci. Model Dev. 8 (9), 2777–2813. https://doi.org/10.5194/gmd-8-2777-2015.
Masselot, Pierre, Sera, Francesco, Schneider, Rochelle, Kan, Haidong, Lavigne, Éric, Stafoggia, Massimo, et al., 2022. Differential mortality risks associated with PM2.5 components: a multi-country, multi-city study. *Epidimiology* 33 (2), S167–S175. https://doi.org/10.1097/EDE.0000000000001455.
Orr, A., Kendall, R.L., Jaffar, Z., Graham, J., Migliaccio, C.T., Knudson, J., et al., 2025. A systematic review and meta-analysis on the association between PM2.5 exposure and increased influenza risk. Front. Epidemiol. 5. https://doi.org/10.3389/fepid.2025.1475141. S. 1475141.
Reuter, M., Dragano, N., Wahrendorf, M., 2020. Working while sick in context of regional unemployment: a Europe-wide cross-sectional study. J. Epidemiol. Community Health. https://doi.org/10.1136/jech-2020-214888.
Rittweger, Jörn, Gilardi, Lorenza, Baltruweit, Maxana, Dally, Simon, Erbertseder, Thilo, Mittag, Uwe, et al., 2022. Temperature and particulate matter as environmental factors associated with seasonality of influenza incidence - an approach using Earth observation-based modeling in a health insurance cohort study from Baden-Württemberg (Germany). Environ. HealthA Global Access Science Source. 21 (1). https://doi.org/10.1186/s12940-022-00927-y. S. 131.
Sangkham, S., Phairuang, W., Sherchan, S.P., Pansakun, N., Munkong, N., Sarndhong, K., et al., 2024. An update on adverse health effects from exposure to PM2.5. Environ. Adv. 18. https://doi.org/10.1016/j.envadv.2024.100603. S. 100603.
Statistisches Landesamt Baden-Württemberg (2025): Bevölkerung Baden-Württembergs am 31. Dezember 2024 nach Alters- und Geburtsjahren. Bevölkerungsfortschreibung auf Basis des Zensus 2022. Stuttgart: Statistisches Landesamt Baden-Württemberg.
Sun, Y., Milando, C.a.W., Spangler, K.R., Wei, Y., Schwartz, J., Dominici, F., et al., 2024. Short term exposure to low level ambient fine particulate matter and natural cause, cardiovascular, and respiratory morbidity among US adults with health insurance: case time series study. In: BMJ (clinical Research Ed.) 384, e076322. https://doi.org/10.1136/bmj-2023-076322.
Tahara, M., Fujino, Y., Yamasaki, K., Oda, K., Kido, T., Sakamoto, N., et al., 2021. Exposure to PM2.5 is a risk factor for acute exacerbation of surgically diagnosed idiopathic pulmonary fibrosis: a case-control study. Respir. Res. 22 (1), S. 80. https://doi.org/10.1186/s12931-021-01671-6.
The Lancet Public Health (2018): Public health and the workplace: a new era dawns. In: *The Lancet. Public health* 3 (11), e508. DOI: 10.1016/S2468-2667(18)30217-2.
Troelstra, Sigrid A., Coenen, Pieter, Boot, Cécile Rl, Janneke, Harting, Kunst, Anton E., Van der Beek, Allard J., 2020. Smoking and sickness absence: a systematic review and meta-analysis. Scand. J. Work Environ. Health 46 (1), 5–18. https://doi.org/10.5271/sjweh.3848.
Vineis, P., Barouki, R., 2022. The exposome as the science of social-to-biological transitions. Environ. Int. 165. https://doi.org/10.1016/j.envint.2022.107312. S. 107312.
WHO World Health Organization (2021): WHO Global Air Quality Guidelines. Particulate Matter (PM2. 5 and PM10), Ozone, Nitrogen Dioxide, Sulfur Dioxide and Carbon Monoxide. 1st ed. Geneva: World Health Organization. Online verfügbar unter https://ebookcentral.proquest.com/lib/kxp/detail.action?docID=30479186.
Wood, S.N., 2017. Generalized additive models. Chapman and Hall/CRC.
Yu, Kexin, Zhang, Qingli, Wei, Yuhao, Chen, Renjie, Kan, Haidong, 2024a. Global association between air pollution and COVID-19 mortality: a systematic review and meta-analysis. The Science of the Total Environment 906. https://doi.org/10.1016/j.scitotenv.2023.167542. S167542.
Yu, W., Xu, R., Ye, T., Abramson, M.J., Morawska, L., Jalaludin, B., et al., 2024b. Estimates of global mortality burden associated with short-term exposure to fine particulate matter (PM2·5). The Lancet. Planetary Health 8 (3), e146–e155. https://doi.org/10.1016/S2542-5196(24)00003-2.
Zhai, X., Wang, J., Sun, J., Xin, L., 2022. PM2.5 induces inflammatory responses via oxidative stress-mediated mitophagy in human bronchial epithelial cells. Toxicol. Res. 11 (1), 195–205. https://doi.org/10.1093/toxres/tfac001.
Zhang, Wei, Bansback, Nick, Anis, Aslam H., 2011. Measuring and valuing productivity loss due to poor health: a critical review. *Soc Sci Med* 72 (2), S. 185–S192. https://doi.org/10.1016/j.socscimed.2010.10.026.

Further reading

Destatis Statistisches Bundesamt (2025a): Earnings and earnings differences. Average gross monthly earnings - Code: 640844. Online verfügbar unter https://www.destatis.de/EN/Themes/Labour/Earnings/Branch-Occupation/Tables/liste-average-gross-monthly-earnings.html#640844.
Destatis Statistisches Bundesamt (2025b): Labor Costs, Non-Wage Labor Costs. Non-Wage Labor Costs in Germany in Euros. Online verfügbar unter https://www.destatis.de/DE/Themen/Arbeit/Arbeitskosten-Lohnnebenkosten/Tabellen/lohnkosten-deutschland.html.